Materials Science & Engineering A 748 (2019) 379–385

Contents lists available at ScienceDirect

Materials Science & Engineering A

journal homepage: www.elsevier.com/locate/msea

Tailoring bimodal grain size structures in nanocrystalline compositionally complex alloys to improve ductility

B. Schuh[a,b,*], R. Pippan[a], A. Hohenwarter[b]

[a] Erich Schmid Institute of Materials Science, Austrian Academy of Sciences, Jahnstraße 12, 8700 Leoben, Austria
[b] Department of Materials Science, Chair of Materials Physics, Montanuniversität Leoben, Jahnstraße 12, 8700 Leoben, Austria

ARTICLE INFO

Keywords:
Tensile tests
Electron microscopy
Nanocrystalline
High entropy alloy
Bimodal microstructures

ABSTRACT

The feasibility of engineering bimodal grain size distributions to achieve superior mechanical properties was explored in two face-centered cubic compositionally complex alloys, namely CrMnFeCoNi and its high-performance subvariant CrCoNi. Therefore both alloys were processed down to the nanocrystalline grain size regime by utilizing high-pressure torsion and subsequently annealed at intermediate temperatures. Especially the CrCoNi alloy is prone to formation of bimodal microstructures and for an annealing treatment at 500 °C for 100 h an excellent combination of ultra-high tensile strength, exceeding 1500 MPa, and decent ductility with elongations to failure of 10% could be achieved.

1. Introduction

High-entropy alloys (HEAs) and compositionally complex alloys (CCAs) are a new class of multi-component metallic materials that have shown outstanding properties, sometimes surpassing conventional alloys and therefore sparking huge interest in the research community [1–6]. Among the most promising candidates are two face-centered-cubic (fcc) alloys with equiatomic compositions, CrMnFeCoNi and CrCoNi. Both alloys exhibit excellent mechanical properties [1,2,7–9], especially at cryogenic temperatures showing high ductility and fracture toughness, as well as yield strengths comparable to many TWIP steels [10,11]. In recent years extensive research has gone into further improving the mechanical strength of these fcc HEAs [12–15]. One feasible approach is granted by extensive grain-refinement, for example achieved by high-pressure torsion (HPT) which commonly produces high-strength materials [16–20]. However, a majority of nanocrystalline (NC) materials, irrespective of the used synthesis process, suffer from a fundamental problem – limited ductility. According to Ma et al. ductility in NC materials is heavily influenced by two aspects [21]: I) A tendency towards a cracking instability/brittle failure, often influenced by sample quality. II) Excessive localized deformation and plastic instabilities due to a low capacity for strain hardening leading to low uniform elongations in uniaxial tensile tests.

Several strategies have been proposed to counteract the problem of low uniform elongation during tensile testing in NC materials, which otherwise could hinder the practical application of such materials in future. The common denominator of these strategies is to raise the low strain hardening rate and therefore delay the onset of necking [22–24]. One straight-forward approach is annealing the material in order to achieve a slightly larger grain size – However, this often results in a considerable loss of strength to gain ductility ("strength-ductility trade off"). Another idea, to achieve better ductility and high strength at the same time, is to tailor a bimodal grain size distribution [22–25]. An example of this can be found in Reference [26]. Wang et al. could impressively increase the strength of coarse-grained copper specimens while retaining elongations to failure of more than 60%, by combining ultrafine grains with a volume fraction of about 25% of larger grains. These results could partly be attributed to the fact that larger grains preferentially accommodate deformation. Another aspect is that the confined grains are under a complex stress state, which is beneficial for dislocation storage and hence strain hardening. Since the CrCoNi alloy is prone to abnormal grain growth, the tailoring of such bi- or multimodal microstructures can be achieved by annealing treatments after HPT processing [27]. In order to explore if the bimodal grain size distribution approach for ductility enhancement in NC CCAs is a feasible approach, the present study was initiated. In the center of interest was the aforementioned ternary equiatomic CrCoNi alloy as well as the CrMnFeCoNi alloy for comparative purposes.

2. Material and methods

Both materials were produced from high-purity elements using arc

* Corresponding author at: Erich-Schmid-Institute of Materials Science, Austrian Academy of Sciences, Jahnstraße 12, 8700 Leoben, Austria.
E-mail addresses: Benjamin.Schuh@oeaw.ac.at (B. Schuh), reinhard.pippan@oeaw.ac.at (R. Pippan), anton.hohenwarter@unileoben.ac.at (A. Hohenwarter).

https://doi.org/10.1016/j.msea.2019.01.073
Received 4 December 2018; Received in revised form 23 January 2019; Accepted 24 January 2019
Available online 25 January 2019

melting and drop casting into copper molds and afterwards subjected to a 24–48 h homogenization treatment at 1200 °C. The ingots were then cold forged and cross rolled with a thickness reduction of approximately 60% at room temperature and subsequently subjected to an annealing treatment at 800 °C for 1 h – for processing details see [1,2,8]. Disks of 8 mm in diameter and 0.8 mm in thickness were machined out of the ingots and deformed via quasi-constrained HPT. 5 rotations were applied for each disk at room-temperature with a pressure of 7.8 GPa. This led to a saturation in grain size within large parts of the disk with a steady state grain size of about 50 nm in both materials [27,28]. Subsequently, both alloys underwent heat treatments at intermediate temperatures in order to achieve bimodal grain size distributions. Microstructural as well as fractographic investigations were performed utilizing a scanning electron microscope (SEM, Zeiss 1525) equipped with an Electron Back Scatter Diffraction (EBSD) system form EDAX. In the bimodal structures the grain size of the coarse-grains (CGs) was determined by EBSD-measurements. Scans were performed with a step size of 70 nm. For the analysis the OIM Analysis 5 software package was used and only data points with a confidence index higher than 0.1 were taken into account [29]. In order to evaluate the size of the coarse grains, only grains larger than 500 nm were considered. High angle grain boundaries were defined as having a minimum misorientation of 15° and Σ3 recrystallization twins were excluded from the analysis. The volume fraction of coarse and nanocrystalline grains was determined by performing a systematic point count method on back-scattered electron micrographs.

In order to evaluate the tensile properties at least 3 samples per microstructural state were tested. Two samples were prepared from each HPT disk with the gauge length of the tensile sample located at a radius of 2 mm and therefore well within the microstructural homogenous saturation area of the HPT disk. Tensile samples had a nominal cross sectional diameter of 500 μm and a gauge length of 2.5 mm and. Tests then were performed utilizing a tensile testing machine from Kammrath and Weiss, at room temperature with a 2 kN load cell and a cross head speed of 2.5 μm/s. For data analysis a MatLab [30] software package was used for automated digital image correlation. All further details on specimen preparation, testing and data evaluation can be found elsewhere [31].

3. Results and discussion

3.1. Investigated microstructures

In the CrCoNi alloy 3 different bimodal grain size distribution were introduced via annealing treatments, see Fig. 1a)-c). In Fig. 1a) it can be seen that an annealing treatment at 550 °C for 10 min resulted in a microstructure consisting of a volume fraction of CGs of 10–20%, which are relatively homogenously embedded in the NC-matrix. Heat treatments at 500 °C for 15 h on the other hand produced a microstructure that consisted of about 70–80% of CGs, see Fig. 1b). Lastly, at 500 °C for 100 h a microstructure consisting predominantly of CGs with small islands of NC grains in between was achieved, Fig. 1c). Considering the results obtained in reference [27], the presence of a minority phase is to be expected for these microstructural states. However, it was demonstrated that this minority phase has a negligible impact on the mechanical properties. This can be interfered from tests of the CrCoNi alloy showing a very similar behavior as a comparable structural material, austenitic 316 L steel, which is a single-phase fcc material with low stacking fault energy (SFE) [27]. Obtaining bi- or multimodal grain size distributions via annealing in the CrMnFeCoNi alloy on the other hand is experimentally more challenging due to its phase instability at intermediate annealing temperatures [28,32–34]. The CrMnFeCoNi alloy only remains a single-phase alloy for annealing temperatures of approximately higher than 800 °C, however pre-experiments showed that at such elevated temperatures even short time anneals (in the range of minutes) led to fully recrystallized, homogenous microstructures. Thus, tailoring bimodal grain size distributions can only be attempted in the temperature range where second phases are formed upon annealing as well. Since long term annealing treatments at intermediate temperatures, such as performed for the CrCoNi alloy, would lead to the formation of a substantial amount of embrittling precipitates in the CrMnFeCoNi alloy, a different annealing procedure was used [28,32,34]. In Fig. 1d) it can be seen that an annealing treatment at 600 °C for 2 min resulted in a very low fraction of CG as well as precipitation of second phases. At 700 °C it is already difficult to achieve bimodal grain size distributions, the fcc-matrix is homogenous and the bimodality is only caused by the precipitation of smaller second phase particles at the grain boundaries. According to the literature the second phases that are formed both at 600 °C and 700 °C should be a Cr-rich tetragonal σ-phase, while additionally at 600 °C a Cr-rich bcc phase can sometimes be found as well [32,34,35]. In Table 1 a brief summary of the volume fraction of the CG portion ($f_{V,CG}$) and the approximate size of the NC grains as well as of the CGs is given. Further microstructural images of various heat treatments performed in a pre-study can be found in the Supplementary Information to demonstrate the difficulty of achieving bimodal grain size microstructures in the CrMnFeCoNi alloy

3.2. Correlation between microstructure and mechanical response

Representative stress-strain curves obtained from tensile testing can be found in Fig. 2 for the CrCoNi alloy and in Fig. 4 for the CrMnFeCoNi alloy. All mechanical properties are summarized in Table 2, where also the reduction of area as an additional measure of ductility was added. In Figs. 2 and 4 as well as Table 2 the mechanical properties of the HPT deformed states and a CG state, with an average grain size of 5–6 μm for both alloys, were added. More information on the mechanical properties and the microstructure of these samples can be found in References [1,2,27,28].

In the 550 °C, 10 min sample the increase in ultimate tensile strength (UTS) from approximately 2067 MPa for the HPT processed state to about 2170 MPa for the heat treated state is accompanied by a decrease in tensile ductility. The total elongation to failure is already low for the HPT processed samples, about 3.9%, and after the heat treatment the total elongation to failure is only 1.4%, with some samples even fracturing in the elastic regime of the test. The fraction of CGs to NC grains is much higher in the 500 °C, 15 h state, as can be seen in Fig. 1b), leading to significantly different mechanical behavior. The UTS is reduced to approximately 1616 MPa, the elongation to failure is increased to about 5.2%. A further increase in the fraction of CG, as seen for an annealing treatment at 500 °C for 100 h (Fig. 1c)) leads to a small decrease in UTS, however, the tensile ductility almost doubles and reaches values of 10%. In brief, two microstructural states show an improved ductility compared to the HPT processed state. However, this increase in tensile ductility is mostly owed to a much more pronounced non-uniform elongation, since in all bimodal samples necking still occurs at considerably low values of uniform elongation similar to the full NC-state (HPT-deformed). Nonetheless, this result is promising for two reasons. Firstly, it demonstrates the feasibility and transferability of bimodal grain size structuring in/to HEAs. Secondly, in a recent review Miracle et al. [3] remarked that if HEAs/CCAs based on 3d-transition elements are to be used as structural material they have to compete with stainless steels. As an example for the excellent mechanical properties HEAs have to overcome he named properties of precipitation-strengthened stainless steels with yield strengths ranging from 1000 to 1400 MPa and a tensile ductility between 2% and 10%. These criteria are met in the 500 °C, 100 h annealing state of the CrCoNi alloy, hence demonstrating that 3d-transition element CCAs can be competitive, given the appropriate microstructure optimization.

While plenty of reports of the beneficial nature of bi- or multi-modal microstructures regarding the mechanical properties exist in the literature, the influence of many microstructural parameters, such as ratio

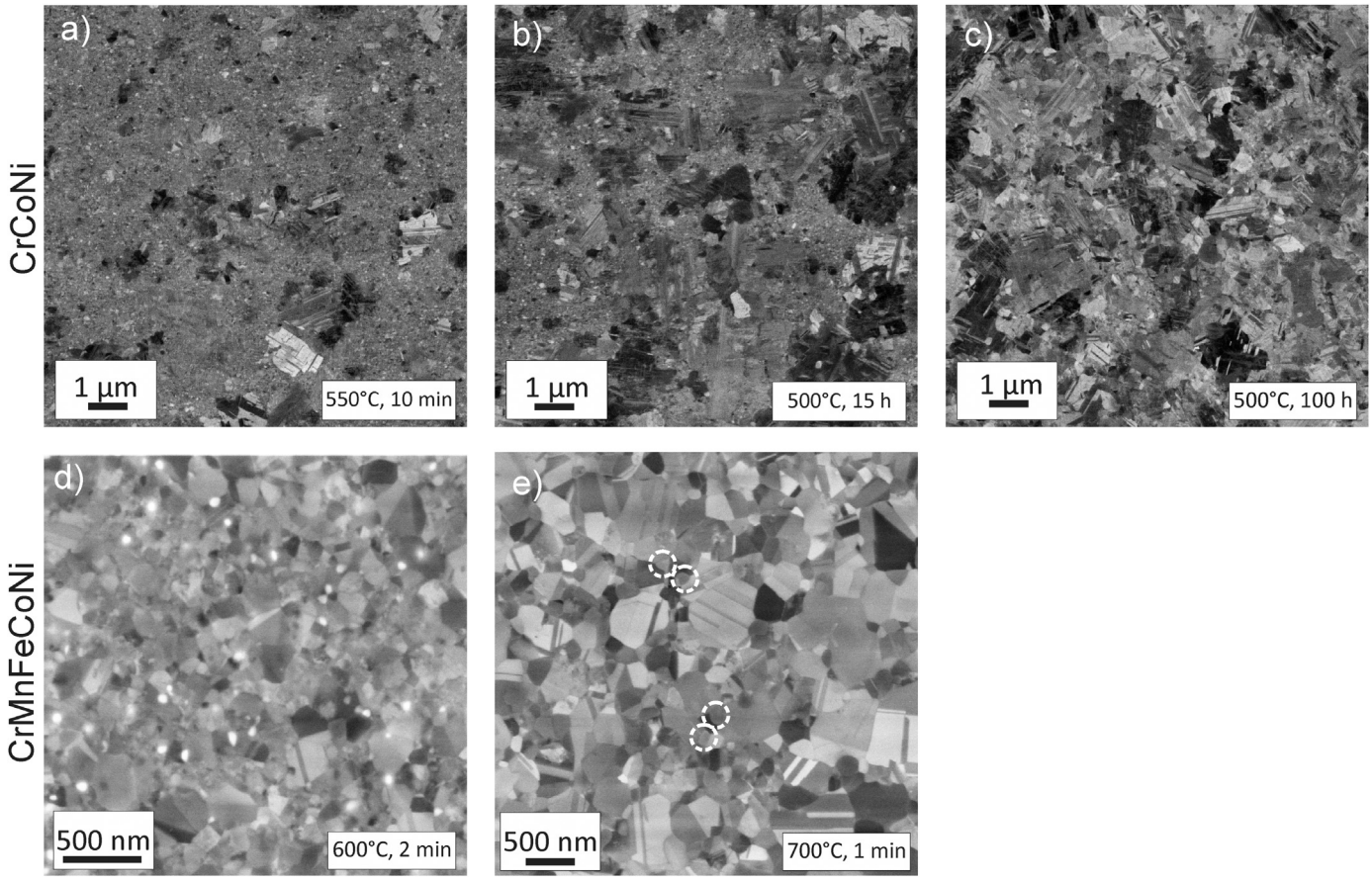

Fig. 1. Back-scattered electron images of the microstructures after annealing treatments of the CrCoNi alloy, a) to c), and the CrMnFeCoNi alloy, d) and e). a) An annealing treatment at 550 °C for 10 min leads to a small fraction of coarse grains (CGs) embedded in a NC grain matrix. b) 15 h of annealing at 500 °C increases the fraction of CGs and CG regions start to coalesce. c) At 500 °C, 100 h only small islands of NC grains remain. For both microstructural states of the CrMnFeCoNi alloy d) and e) the formation of second phases can be observed, in e) they are marked by white circles due to their poor visibility. While a 600 °C, 2 min heat treatment leads to a pronounced bimodal grain size distribution, at 700 °C for 1 min the microstructure is already quite homogenous.

Table 1
Summary of microstructural parameters, $f_{V,CG}$ is the volume fraction of CGs.

	Sample	$f_{V,CG}$ (%)	CG	NC
CrCoNi	550 °C, 10 min	16.3 ± 7.5	1.2 ± 0.4 µm	< 100 nm
	500 °C, 15 h	76.3 ± 3.1	1.8 ± 0.6 µm	< 100 nm
	500 °C, 100 h	97.6 ± 0.8	2.0 ± 0.5 µm	< 100 nm
CrMnFeCoNi	600 °C, 2 min	2.5 ± 0.2	< 300 nm	< 100 nm
	700 °C, 1 min	No bimodality - Grain size of ~ 400 nm		

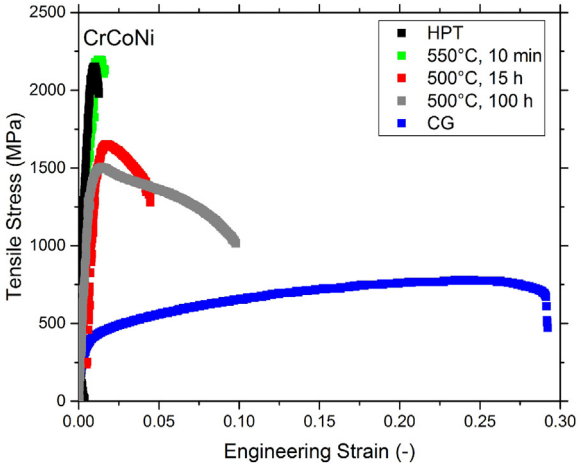

Fig. 2. Representative tensile stress-strain curves of different microstructural states of the CrCoNi alloy.

of large to small grains, grain shape and distribution is still controversially discussed [26,36–38]. An in-depth study on bimodal Cu revealed that, both, yield strength and uniform elongation follow the rule-of-mixtures [37], which can be supported by simulation and modelling approaches [39,40]. However, Zhao et al. also noted that positive and negative deviations from the rule-of-mixtures, are frequently reported, which may be attributed to size-ratio differences between small and large grains but also the spatial distribution [37]. For instance, Wang et al. [26] reported a strength-ductility combination much superior to what is suggested by the rule-of-mixtures at a volume fraction of CG of about 25%. Another study on bimodal aluminum alloys on the other hand shows diminishing returns when increasing the fraction of CG beyond a certain point – This was explained by the fact that when a certain threshold volume fraction of CG areas is reached, where they start to coalesce, their ability to act as crack arrestors saturates [41].

Ideally, in bimodal structures the largest grains are constrained by the surrounding finer grains and yield first during loading. As the load further rises, the stress concentration caused by dislocation pile-ups in the CGs increases as well, until a critical value is reached and slip systems in the NC grains are activated, causing a load transfer between the CG/NC interface and plastic deformation in the NC grains [42]. Hence, while the mechanical behavior of bimodal structures is often only discussed with respect to the significance of the CG volume

Table 2
Summarized mechanical properties of the tested microstructural states of the CrCoNi and CrMnFeCoNi alloy.

Microstructural state		Ultimate tensile strength (MPa)	Elongation to failure (%)	Yield strength $\sigma_{0.2}$ (MPa)	Area reduction (%)
CrCoNi	CG	784 ± 42	30 ± 2	402 ± 21	84 ± 11
	HPT	2067 ± 153	3.9 ± 1.5	1901 ± 114	22 ± 8
	550 °C, 10 min	2170 ± 98	1.4 ± 0.3	*	*
	500 °C, 15 h	1616 ± 38	5.2 ± 0.2	1530 ± 83	46 ± 13
	500 °C, 100 h	1520 ± 15	10 ± 0.2	1452 ± 35	58 ± 2
CrMnFeCoNi	CG	641 ± 10	25 ± 2	329 ± 30	76 ± 6
	HPT	1924 ± 124	3.2 ± 1.3	1787 ± 200	30 ± 13
	600 °C, 2 min	1669 ± 266	1.5 ± 0.3	*	*
	700 °C, 1 min	1216 ± 148	5.4 ± 1.5	1207 ± 151	53 ± 5

*Not all specimens yielded before fracture.

fraction, it is clear that grain size has an equally important impact. In consideration how bimodal structures are deforming, the further decrease in yield strength observed between the CrCoNi systems for the annealing states of 500 °C for 15 h and 100 h should therefore primarily be caused by the difference in their CG sizes and not the difference in their volume fractions. This is substantiated by the findings of Magee et al. who reported a saturation effect of the CG volume fraction regarding the yield strength once the CG areas start to coalesce. Transferred to the current case, this means that the further increase in CG volume fraction between the 500 °C for 15 h and 100 h annealing state would no longer lead to a significant change in strength, since even in the 15 h state CG regions are already strongly interconnected [41].

The reason for the observed phenomena in the 550 °C, 10 min, where higher mechanical strengths are achieved despite the presence of CGs cannot yet be fully explained and future investigations are needed. The main cause most likely lies in the strong intersection of CGs by recrystallization twins, leading to significantly smaller substructures than the overall grain size suggests, see Fig. 3. Additional strengthening could be provided by a “hardening by annealing” phenomenon frequently observed in NC metals [43,44] including the CrCoNi and the CrMnFeCoNi alloy [27,28]. The cause of such “hardening by annealing” phenomena is still controversially discussed in the literature, but they seem to be linked to a certain threshold grain size [44]. A popular explanation is that annealing treatment of NC structures lead to a rapid dislocation annihilation at the readily available grain boundaries, which results in a depletion of mobile dislocations in the grain interior. If subsequently plastic deformation is to be realized, dislocation emission from grain boundary sources is necessary. However, according to Ma et al. such an annealing treatment should also cause a relaxation of the grain boundaries, which makes dislocation emission more difficult [45]. Another explanation for the phenomenon might be related to grain boundary segregation and a more difficult dislocation emission caused by solute-drag effects [46].

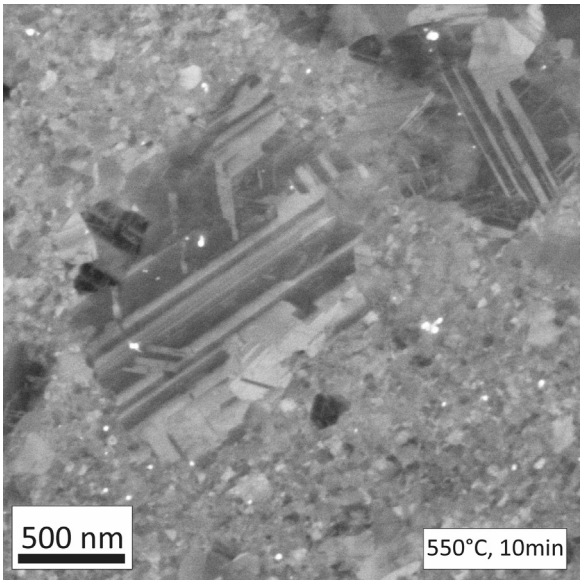

Fig. 3. Recrystallization twins leading to a strong intersection of the CG in the CrCoNi alloy.

Besides distinctive changes in the strength levels of the differently heat-treated CrCoNi samples, the ductility is clearly affected as well. Focusing only on the uniform elongation, the samples with bimodal microstructures show relatively low values compared to the CG reference state with grain sizes around 6 µm. This is a result of a low strain hardening rate which leads to a quick damage localization. This low strain hardening rate despite the presence of CG likely originates from the fact that mechanical twinning is not very pronounced in the CG regions of the bimodal structures with grain sizes around 1 µm (see Table 1). In low SFE metals, such as both, the CrCoNi and CrMnFeCoNi alloy, the twinning propensity is strongly dependent on the grain size [47]. This is well exemplified by a study on a MP35N (35% Co 35% Ni 20% Cr 10% Mo) alloy, where a high twin density was observed in microstructures with a grain size of about 40 µm but no twinning occured after deformation for an average grain size of 1 µm [47]. Another example proving that bimodal microstructures do not necessarily lead to beneficial properties is exemplified by another low SFE alloy, 316 L steel [48]. Given the average grain size of the CG in the CrCoNi alloy in this investigation (in the range of 1 µm), it is reasonable to assume that the propensity for mechanical twinning and hence the strain hardening rate is strongly reduced in comparison to studies performed on coarser-grained CrCoNi samples (grain-size ~ 6 µm) [2]. While the strain hardening rate is too low to sustain uniform elongation, the larger substructures in the CG still provide better capabilities for dislocation storage compared to the NC state, which is one factor leading to an improved non-uniform elongation and area reduction especially observed in the 500 °C, 100 h annealing state. In addition, the damage accumulation is postponed by the CG-fraction as it can be partly inferred from fractographic investigation (see later).

The results of the annealing treatments of the CrMnFeCoNi alloy are presented in Fig. 4. After annealing samples at 600 °C for 2 min usually fail prematurely in the elastic regime of the tensile test, similarly to what has been reported in the literature for 1 h annealed samples [28]. However, for the 700 °C, 1 min heat treatment some ductility is restored at the cost of a considerable loss of strength. Due to the thermodynamic instability of the alloy the formation of additional phases during heat-treatments is unavoidable. Therefore, the results for the 600 °C state show a deterioration of the deformation behavior compared to the HPT-state. Only for the 700 °C, 1 min annealing state an improvement in ductility was found, as the presence of second phase particles is strongly reduced, Fig. 1e). The negative effect of additional phases could be circumvented by using other processing routes which could have the potential to achieve bimodal microstructures without the formation of the second phases, for instance via consolidation of both CG and NC powder blends [42,49,50]. Additionally, another way to achieve

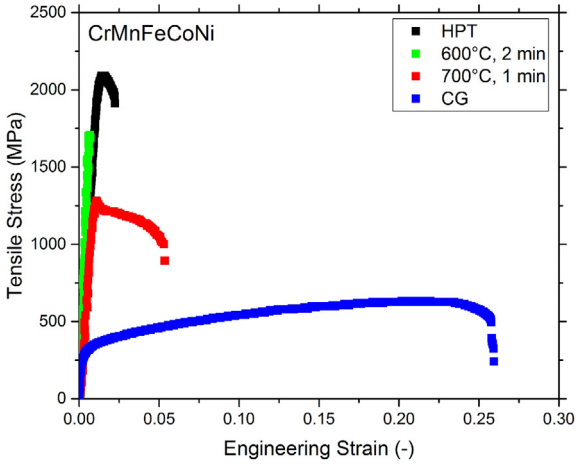

Fig. 4. Representative tensile stress-strain curves of different microstructural states of the CrMnFeCoNi alloy.

excellent strength-ductility combinations in homogenous single-phase materials was demonstrated recently. Tian et al. [51] subjected HPT-processed Cu to post annealing treatments and while for grain sizes of approximately 300 nm a yield drop phenomenon and a quick damage localization and subsequent failure was observed, for slightly larger grains of about 500 nm excellent mechanical properties were reported. The main difference is that, while the 500 nm microstructural state also showed a yield drop phenomenon, the strain hardening capability is high enough that the Lüders band can propagate throughout the material, leading to a very large Lüders strain. Similarly, the 700 °C, 1 min CrCoFeMnNi alloy also shows a yield drop phenomenon, see Fig. 4. This yield phenomenon likely originates in the formation of a Lüders band that is not propagating throughout the sample due to an insufficient work hardening rate and leads to instant localization. Hence, it would be interesting to attempt if such an extensive Lüders strain could be reached in the CrCoFeMnNi alloy by tailoring slightly larger grain sizes as well.

3.3. Fractography

In Fig. 5a) to c) representative fracture images of the CrCoNi alloy annealed at 550 °C for 10 min and at 500 °C for 15 h and 100 h, respectively, can be seen. Despite the fact that all microstructural states show ductile fractures with dimple formation the amount of ductility is very different. In detail, especially in b) and c) large and deep dimples formed around intermetallic inclusions can be observed. From microstructurally uniform samples it is known that the failure mechanism typical for CG-structures involves the void initiation and formation from inclusions leading to these pronounced deep dimples during failure as presented in Fig. 5b) (macrodimples). In NC-materials void formation is controlled by triple junctions and grain boundaries acting as initiation points leading to shallow dimples in the range of the grain size or somewhat larger (micro- or nano-dimples) [52]. As especially Fig. 5b) shows, the final fracture of the sample is controlled by the coalescence of the macrovoids forming large and deep dimples stemming from the CG-fraction. This requires more plastic deformation than the formation of the micro/nanovoids and delays final failure of the sample. As a result, while the as processed and 550 °C, 10 min sample fractures with little macroscopic plasticity, the 500 °C, 15 h and 100 h sample with high CG-fractions show much higher values for the elongation to failure. On the macroscopic level for the brittle case (550 °C, 10 min) shear fracture is typical, whereas in the more ductile case (500 °C 15 and 100 h) a cup-and-cone fracture prevails, see Fig. 6.

Fig. 7 Depicts SEM fractographs of the CrMnFeCoNi alloy that underwent annealing treatments at 600 °C for 2 min, a), and 700 °C for 1 min, b). Despite the precipitation of brittle second phases mainly on the grain boundaries, both materials fail at first sight again in a ductile fracture mode with dimple formation. In Fig. 7a) the dimples are small and shallow, whereas in Fig. 7b) it can be clearly observed that dimples form around the second phase precipitates that are larger and therefore consume considerably more plastic deformation, which is also well reflected when comparing the maximum elongation before failure between the two annealing states. Since the number of the precipitates is very large compared to the CoCrNi-alloy after 100 h heat-treatments, they coalesce earlier and lead to a lower total elongation before failure. The macroscopic behavior is the same as in the CrCoNi alloy: In the brittle case (600 °C, 2 min), shear fracture occurs whereas in the more ductile specimen (700 °C, 1 min) a cup and cone fracture was found.

4. Conclusions

In this study bimodal grain size distributions were induced via heat-treatments in two nanocrystalline compositionally complex alloys, CrMnFeCoNi and CrCoNi, with the aim to enhance their ductility. In case of the CrMnFeCoNi alloy it was found that tailoring bimodal grain size distributions is experimentally very challenging to achieve due to the thermodynamic instability of the alloy, leading to multiphase structures with embrittling phases in a large temperature window. Therefore, the combination of SPD-processing and annealing does not seem to be a feasible way to achieve supreme tensile properties in this alloy.

In contrast, in the CrCoNi alloy a twofold increase in ductility was

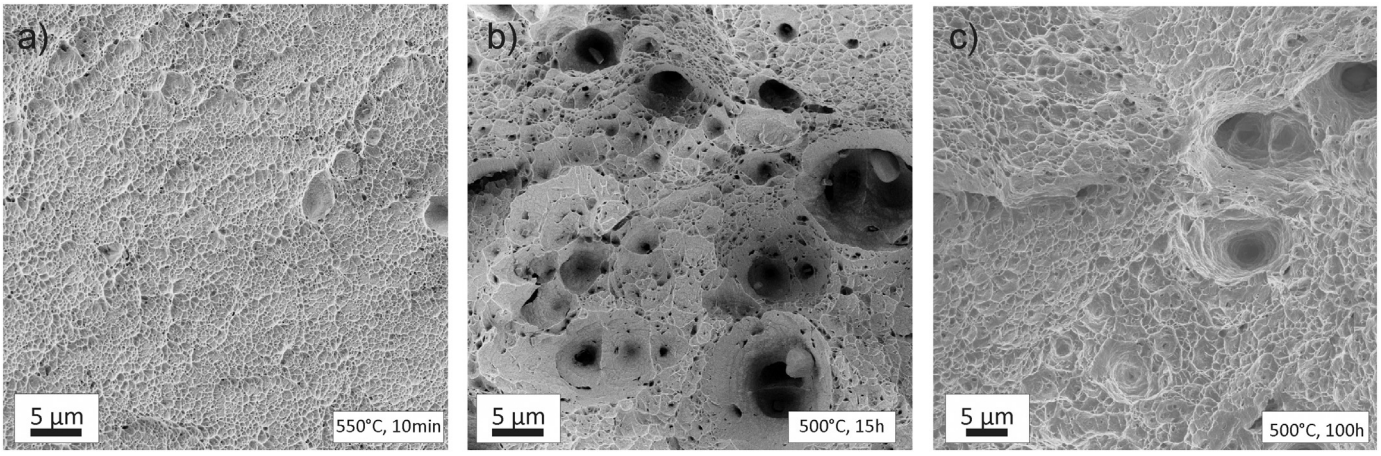

Fig. 5. In a) to c) the fracture images of CrCoNi tensile samples annealed at 550 °C for 10 min and at 500 °C for 15 h and 100 h can be seen. All of them feature a ductile fracture surface with dimple formation.

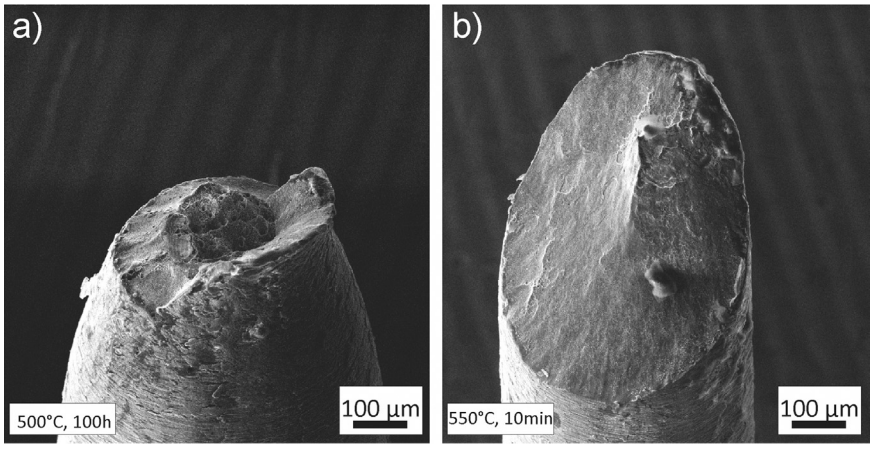

Fig. 6. Macroscopic fracture images of the CrCoNi alloy. a) shows the ductile 500 °C, 100 h annealing state with a cup-and-cone fracture. b) Flat shear fracture of the 500 °C, 10 min annealed samples.

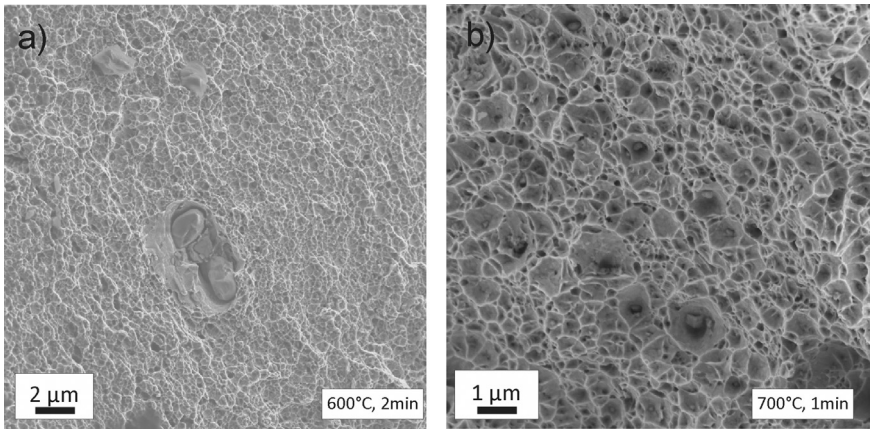

Fig. 7. Despite the formation of second phases during annealing (600 °C, 2 min in a) and 700 °C, 1 min in b)) of the CrMnFeCoNi alloy the fracture mode remains ductile. In b) the dimple formation around these second phases can be observed.

achieved via grain size engineering. Further optimization of the heat treatment might yield microstructural states with both high tensile strength and a high strain hardening rate so that uniform elongation can be sustained for large strains during deformation. A feasible way to achieve this might be by increasing the size of the CG grains. While this could provoke somewhat lower yield strengths, larger grains should promote a better strain hardening rate through a higher mechanical twinning propensity.

Acknowledgments

This work was supported by the Austrian Science Fund FWF in the framework of Research Project P26729-N19. Funding of this work has also been provided by the European Research Council under ERC Grant Agreement No. 340185 USMS. The authors would like to thank Prof. Easo P. George for providing the material necessary to perform this study.

Data availability statement

The raw/processed data are available from the corresponding author upon request.

Appendix A. Supporting information

Supplementary data associated with this article can be found in the online version at doi:10.1016/j.msea.2019.01.073.

References

[1] B. Gludovatz, A. Hohenwarter, D. Catoor, E.H. Chang, E.P. George, R.O. Ritchie, A fracture-resistant high-entropy alloy for cryogenic applications, Science 345 (2014) 1153–1158, https://doi.org/10.1126/science.1254581.
[2] B. Gludovatz, A. Hohenwarter, K.V.S. Thurston, H. Bei, Z. Wu, E.P. George, R.O. Ritchie, Exceptional damage-tolerance of a medium-entropy alloy CrCoNi at cryogenic temperatures, Nat. Commun. 7 (2016) 10602, https://doi.org/10.1038/ncomms10602.
[3] D.B. Miracle, O.N. Senkov, A critical review of high entropy alloys and related concepts, Acta Mater. 122 (2017) 448–511, https://doi.org/10.1016/j.actamat.2016.08.081.
[4] Y. Zhang, T.T. Zuo, Z. Tang, M.C. Gao, K.A. Dahmen, P.K. Liaw, Z.P. Lu, Microstructures and properties of high-entropy alloys, Prog. Mater. Sci. 61 (2014) 1–93, https://doi.org/10.1016/j.pmatsci.2013.10.001.
[5] O.N. Senkov, G.B. Wilks, D.B. Miracle, C.P. Chuang, P.K. Liaw, Refractory high-entropy alloys, Intermetallics 18 (2010) 1758–1765, https://doi.org/10.1016/j.intermet.2010.05.014.
[6] J.-P. Couzinié, G. Dirras, Body-centered cubic high-entropy alloys: from processing to underlying deformation mechanisms, Mater. Charact. 147 (2019) 533–544, https://doi.org/10.1016/J.MATCHAR.2018.07.015.
[7] B. Gludovatz, E.P. George, R.O. Ritchie, Processing, microstructure and mechanical properties of the CrMnFeCoNi high-entropy alloy, JOM 67 (2015) 2262–2270, https://doi.org/10.1007/s11837-015-1589-z.
[8] F. Otto, A. Dlouhý, C. Somsen, H. Bei, G. Eggeler, E.P. George, The influences of temperature and microstructure on the tensile properties of a CoCrFeMnNi high-entropy alloy, Acta Mater. 61 (2013) 5743–5755, https://doi.org/10.1016/j.actamat.2013.06.018.
[9] G. Laplanche, A. Kostka, C. Reinhart, J. Hunfeld, G. Eggeler, E.P. George, Reasons for the superior mechanical properties of medium-entropy CrCoNi compared to high-entropy CrMnFeCoNi, Acta Mater. 128 (2017) 292–303, https://doi.org/10.1016/j.actamat.2017.02.036.
[10] B.C. De Cooman, Y. Estrin, S.K. Kim, Twinning-induced plasticity (TWIP) steels, Acta Mater. 142 (2018) 283–362, https://doi.org/10.1016/j.actamat.2017.06.046.
[11] O. Grässel, L. Krüger, G. Frommeyer, L.W. Meyer, High strength Fe-Mn-(Al, Si)

TRIP/TWIP steels development - properties - application, Int. J. Plast. 16 (2000) 1391–1409, https://doi.org/10.1016/S0749-6419(00)00015-2.
[12] N.D. Stepanov, D.G. Shaysultanov, R.S. Chernichenko, N.Y. Yurchenko, S.V. Zherebtsov, M.A. Tikhonovsky, G.A. Salishchev, Effect of thermomechanical processing on microstructure and mechanical properties of the carbon-containing CoCrFeNiMn high entropy alloy, J. Alloy. Compd. 693 (2017) 394–405, https://doi.org/10.1016/j.jallcom.2016.09.208.
[13] N.D. Stepanov, D.G. Shaysultanov, R.S. Chernichenko, D.M. Ikornikov, V.N. Sanin, S.V. Zherebtsov, Mechanical properties of a new high entropy alloy with a duplex ultra-fine grained structure, Mater. Sci. Eng. A 728 (2018) 54–62, https://doi.org/10.1016/j.msea.2018.04.118.
[14] J.B. Seol, J.W. Bae, Z. Li, J. Chan Han, J.G. Kim, D. Raabe, H.S. Kim, Boron doped ultrastrong and ductile high-entropy alloys, Acta Mater. 151 (2018) 366–376, https://doi.org/10.1016/j.actamat.2018.04.004.
[15] Z. Li, C.C. Tasan, K.G. Pradeep, D. Raabe, A TRIP-assisted dual-phase high-entropy alloy: grain size and phase fraction effects on deformation behavior, Acta Mater. 131 (2017) 323–335, https://doi.org/10.1016/j.actamat.2017.03.069.
[16] R. Pippan, S. Scheriau, A. Hohenwarter, M. Hafok, Advantages and limitations of HPT: a review, Mater. Sci. Forum 584–586 (2008) 16–21, https://doi.org/10.4028/www.scientific.net/MSF.584-586.16.
[17] R. Pippan, S. Scheriau, A. Taylor, M. Hafok, A. Hohenwarter, A. Bachmaier, Saturation of fragmentation during severe plastic deformation, Annu. Rev. Mater. Res. 40 (2010) 319–343, https://doi.org/10.1146/annurev-matsci-070909-104445.
[18] R.Z. Valiev, Nanostructuring of metals by severe plastic deformation for advanced properties, Nat. Mater. 3 (2004) 511–516, https://doi.org/10.1038/nmat1180.
[19] R.Z. Valiev, R.K. Islamgaliev, I.V. Alexandrov, Bulk nanostructured materials from severe plastic deformation, Prog. Mater. Sci. 45 (2000) 103–189, https://doi.org/10.1016/S0079-6425(99)00007-9.
[20] A.P. Zhilyaev, T.G. Langdon, Using high-pressure torsion for metal processing: fundamentals and applications, Prog. Mater. Sci. 53 (2008) 893–979, https://doi.org/10.1016/j.pmatsci.2008.03.002.
[21] E. Ma, Instabilities and ductility of nanocrystalline and ultrafine-grained metals, Scr. Mater. 49 (2003) 663–668, https://doi.org/10.1016/S1359-6462(03)00396-8.
[22] E. Ma, Eight routes to improve the tensile ductility of bulk nanostructured metals and alloys, JOM 58 (2006) 49–53, https://doi.org/10.1007/s11837-006-0215-5.
[23] Y. Zhao, Y. Zhu, E.J. Lavernia, Strategies for improving tensile ductility of bulk nanostructured materials, Adv. Eng. Mater. 12 (2010) 769–778, https://doi.org/10.1002/adem.200900335.
[24] Y.M. Wang, E. Ma, Three strategies to achieve uniform tensile deformation in a nanostructured metal, Acta Mater. 52 (2004) 1699–1709, https://doi.org/10.1016/j.actamat.2003.12.022.
[25] Y.M. Wang, E. Ma, M.W. Chen, Enhanced tensile ductility and toughness in nanostructured Cu, Appl. Phys. Lett. 80 (2002) 2395–2397, https://doi.org/10.1063/1.1465528.
[26] Y. Wang, M. Chen, F. Zhou, E. Ma, High tensile ductility in a nanostructured metal, Nature 419 (2002) 912–915, https://doi.org/10.1038/nature01133.
[27] B. Schuh, B. Völker, J. Todt, K.S. Kormout, N. Schell, A. Hohenwarter, Influence of annealing on microstructure and mechanical properties of a nanocrystalline CrCoNi medium-entropy alloy, Materials 11 (2018), https://doi.org/10.3390/ma11050662.
[28] B. Schuh, F. Mendez-Martin, B. Völker, E.P. George, H. Clemens, R. Pippan, A. Hohenwarter, Mechanical properties, microstructure and thermal stability of a nanocrystalline CoCrFeMnNi high-entropy alloy after severe plastic deformation, Acta Mater. 96 (2015) 258–268, https://doi.org/10.1016/j.actamat.2015.06.025.
[29] OIM Analysis v5,EDAX, ⟨https://www.edax.com/products/ebsd/oim-analysis⟩. Last accessed: 01/2019.
[30] MathWorks, MatLab, ⟨https://de.mathworks.com/⟩. Last accessed: 08/2018.
[31] G.B. Rathmayr, A. Bachmaier, R. Pippan, Development of a new testing procedure for performing tensile tests on specimens with sub-millimetre dimensions, J. Test. Eval. 41 (2013) 1–12, https://doi.org/10.1520/JTE20120175.
[32] F. Otto, A. Dlouhý, K.G. Pradeep, M. Kubênová, D. Raabe, G. Eggeler, E.P. George, Decomposition of the single-phase high-entropy alloy CrMnFeCoNi after prolonged anneals at intermediate temperatures, Acta Mater. 112 (2016) 40–52, https://doi.org/10.1016/j.actamat.2016.04.005.
[33] E.J. Pickering, R. Muñoz-Moreno, H.J. Stone, N.G. Jones, Precipitation in the equiatomic high-entropy alloy CrMnFeCoNi, Scr. Mater. 113 (2016) 106–109, https://doi.org/10.1016/j.scriptamat.2015.10.025.
[34] N.D. Stepanov, D.G. Shaysultanov, M.S. Ozerov, S.V. Zherebtsov, G.A. Salishchev, Second phase formation in the CoCrFeNiMn high entropy alloy after recrystallization annealing, Mater. Lett. 185 (2016) 1–4, https://doi.org/10.1016/j.matlet.2016.08.088.
[35] H. Shahmir, T. Mousavi, J. He, Z. Lu, M. Kawasaki, T.G. Langdon, Microstructure and properties of a CoCrFeNiMn high-entropy alloy processed by equal-channel angular pressing, Mater. Sci. Eng. A 705 (2017) 411–419, https://doi.org/10.1016/j.msea.2017.08.083.
[36] V.L. Tellkamp, E.J. Lavernia, A. Melmed, Mechanical behavior and microstructure of a thermally stable bulk nanostructured Al alloy, Metall. Mater. Trans. A 32 (2001) 2335–2343, https://doi.org/10.1007/s11661-001-0207-6.
[37] Y. Zhao, T. Topping, Y. Li, E.J. Lavernia, Strength and ductility of bi-modal Cu, Adv. Eng. Mater. 13 (2011) 865–871, https://doi.org/10.1002/adem.201100019.
[38] Y. Zhao, T. Topping, J.F. Bingert, J.J. Thornton, A.M. Dangelewicz, Y. Li, W. Liu, Y. Zhu, Y. Zhou, E.J. Lavernia, High tensile ductility and strength in bulk nanostructured nickel, Adv. Mater. 20 (2008) 3028–3033, https://doi.org/10.1002/adma.200800214.
[39] S.P. Joshi, K.T. Ramesh, B.Q. Han, E.J. Lavernia, Modeling the constitutive response of bimodal metals, Metall. Mater. Trans. A 37 (2006) 2397–2399, https://doi.org/10.1007/BF02586214.
[40] B. Raeisinia, C.W. Sinclair, W.J. Poole, C.N. Tomé, On the impact of grain size distribution on the plastic behaviour of polycrystalline metals, Model. Simul. Mater. Sci. Eng. 16 (2008) 025001, https://doi.org/10.1088/0965-0393/16/2/025001.
[41] A. Magee, L. Ladani, T.D. Topping, E.J. Lavernia, Effects of tensile test parameters on the mechanical properties of a bimodal Al-Mg alloy, Acta Mater. 60 (2012) 5838–5849, https://doi.org/10.1016/j.actamat.2012.07.024.
[42] Y. Li, Z. Zhang, R. Vogt, J.M. Schoenung, E.J. Lavernia, Boundaries and interfaces in ultrafine grain composites, Acta Mater. 59 (2011) 7206–7218, https://doi.org/10.1016/j.actamat.2011.08.005.
[43] X. Huang, N. Hansen, N. Tsuji, Hardening by annealing and softening by deformation in nanostructured metals, Science 312 (2006) 249–251, https://doi.org/10.1126/science.1124268.
[44] O. Renk, A. Hohenwarter, B. Schuh, J.H. Li, R. Pippan, Hardening by annealing: insights from different alloys, IOP Conf. Ser. Mater. Sci. Eng. 89 (2015) 012043, https://doi.org/10.1088/1757-899X/89/1/012043.
[45] E. Ma, T.D. Shen, X.L. Wu, Nanostructured metals: less is more, Nat. Mater. 5 (2006) 515–516, https://doi.org/10.1038/nmat1671.
[46] R.Z. Valiev, N.A. Enikeev, M.Y. Murashkin, V.U. Kazykhanov, X. Sauvage, On the origin of the extremely high strength of ultrafine-grained Al alloys produced by severe plastic deformation, Scr. Mater. 63 (2010) 949–952, https://doi.org/10.1016/j.scriptamat.2010.07.014.
[47] E. El-Danaf, S.R. Kalidindi, R. Doherty, Influence of grain size and stacking fault energy on deformation twinning in fcc metals, Metall. Mater. Trans. A 30 (1999) 1223–1233.
[48] O. Renk, A. Hohenwarter, R. Pippan, Cyclic deformation behavior of a 316L austenitic stainless steel processed by high pressure torsion, Adv. Eng. Mater. 14 (2012) 948–954, https://doi.org/10.1002/adem.201200015.
[49] G.J. Fan, H. Choo, P.K. Liaw, E.J. Lavernia, Plastic deformation and fracture of ultrafine-grained Al-Mg alloys with a bimodal grain size distribution, Acta Mater. 54 (2006) 1759–1766, https://doi.org/10.1016/j.actamat.2005.11.044.
[50] Y. Zhang, S. Sabbaghianrad, H. Yang, T.D. Topping, T.G. Langdon, E.J. Lavernia, J.M. Schoenung, S.R. Nutt, Two-Step, SPD processing of a trimodal Al-based nanocomposite, Metall. Mater. Trans. A 46 (2015) 5877–5886, https://doi.org/10.1007/s11661-015-3151-6.
[51] Y.Z. Tian, S. Gao, L.J. Zhao, S. Lu, R. Pippan, Z.F. Zhang, N. Tsuji, Remarkable transitions of yield behavior and Lüders deformation in pure Cu by changing grain sizes, Scr. Mater. 142 (2018) 88–91, https://doi.org/10.1016/j.scriptamat.2017.08.034.
[52] A. Hohenwarter, R. Pippan, Fracture and fracture toughness of nanopolycrystalline metals produced by severe plastic deformation, Philos. Trans. R. Soc. A 373 (2015) 20140366, https://doi.org/10.1098/rsta.2014.0366.